Current Science
CS 5 (2), 1847-1855 (2025)
**Received** 20 **Jan** 2025 | **Revised** 21 **Feb** 2025 | **Accepted** 18 **March**. 2025 | **Online Available** 16 **April** 2025
https://doi.org/ 10.52845/CS/2025-5-2-47

Current Science

Current Science

OPEN ACCESS

ISSN(O)2795-8639

**ORIGINAL ARTICLE**

# Finite Element Analysis of PFNA and PFNA Combined with Locking Plate in the Treatment of Femoral Intertrochanteric Fractures with Lateral Wall Fracture

**Long Zhou[1#], Liang Wang[1], Rui Xu[2], Yidong Bao[2], Shuangjian He[1]***

**[1]Department of Orthopedics, Suzhou Hospital, Affiliated Hospital of Medical School, Nanjing University, Suzhou, Jiangsu 215163, P.R. China**

**[2]College of Mechanical and Electrical Engineering, Nanjing University of Aeronautics and Astronautics, Nanjing, Jiangsu 210016, P.R. China**

**[*]Corresponding Author: Shuangjian He**

## Abstract

**Objective:** This study aimed to compare the biomechanical characteristics of Proximal Femoral Nail Antirotation (PFNA) and PFNA combined with Proximal Humerus Locking Plate (PHLP) in the treatment of femoral intertrochanteric fractures with lateral wall fractures using finite element analysis. The biomechanical strength, stress distribution, and displacement patterns of the two internal fixation methods were evaluated.

**Methods:** A three-dimensional finite element model of the femur, PFNA, and PHLP was constructed based on CT scan data from a healthy middle-aged female patient. A simulated AO 31-A3.3 femoral intertrochanteric fracture was created, and two internal fixation models (PFNA and PFNA+PHLP) were assembled. The von Mises stress and displacement distributions were analyzed under static and dynamic loading conditions.

**Results:** Compared to PFNA , PFNA+PHLP fixation reduced the maximum von Mises stress by approximately 40%, with minimal changes in maximum displacement. Stress at the fracture site and main nail decreased significantly, particularly at the main nail (reduction of 40%). The von Mises stress in the femoral head, femoral neck, medial wall, and spiral blade showed minimal changes. The total displacement of the femoral head, femoral neck, lateral wall, and spiral blade in the PFNA+PHLP model decreased slightly but not significantly.

**Conclusion:** PFNA+PHLP fixation demonstrates higher fixation strength and more reasonable stress distribution compared to PFNA in the treatment of femoral intertrochanteric fractures with lateral wall fractures.

**Keywords:** femoral intertrochanteric fracture, femoral lateral wall, intramedullary nail, locking plate, finite element analysis

## Introduction

Femoral intertrochanteric fractures are among the most common hip fractures in the elderly population. Despite a high rate of fracture healing, postoperative functional outcomes are often unsatisfactory. Many patients fail to regain their pre-fracture activity levels, which is influenced by factors such as their overall physical condition, the type of fracture, and the choice of internal fixation method [1, 2]. The lateral wall, anatomically defined as the lateral cortex of the proximal femur extending between the vastus lateralis ridge (below the apex of the greater trochanter) and the midpoint of the lesser trochanter, plays a critical role in fracture stability [3]. An intact lateral wall provides essential support for proximal bone fragments and the

internal fixation spiral blade, promoting bone stabilization, reducing stress on the implant, and lowering the risk of fixation failure [4-6]. Additionally, the lateral wall serves as the attachment site for the gluteus medius and gluteus minimus muscles. Disruption of the lateral wall, especially when accompanied by reduction failure, can significantly compromise the soft tissue balance and stability of the hip joint. Consequently, there is growing interest among scholars in reconstructing the lateral wall to restore stability and function [7, 8].

Femoral intertrochanteric fractures with lateral wall involvement are inherently unstable. The use of Proximal Femoral Nail Antirotation (PFNA) fixation in such cases is associated with complications such as coxa vara, implant loosening, and cut-out, leading to fixation failure [9, 10]. To address these challenges, some clinicians have explored the use of locking plates to reconstruct the lateral femoral wall. This approach aims to enhance early stability, improve mechanical load transfer in the proximal femur, and restore the balance and stability of the hip joint's soft tissues. Comparative studies have demonstrated that lateral wall reconstruction with a locking plate offers significant advantages over PFNA fixation, including shorter fracture healing times, earlier weight-bearing, and improved hip joint function [11]. However, there is a paucity of biomechanical studies comparing these two fixation methods, resulting in a lack of foundational data to support clinical decision-making.

In this study, finite element analysis was employed to evaluate the stress and displacement distributions of two internal fixation models—PFNA and PFNA combined with a Proximal Humerus Locking Plate (PHLP)—under both static and dynamic conditions. The results confirm that PFNA+PHLP fixation provides superior fixation strength and more favorable stress distribution compared to PFNA, offering valuable theoretical support for the clinical treatment of femoral intertrochanteric fractures with lateral wall fractures.

## 2. Material and Methods

### 2.1 Femoral CT data

A 57-year-old female volunteer (weight: 60 kg) with no history of medical or surgical conditions, limb disabilities, or trauma was selected for this study. A 64-slice spiral CT scanner was used to acquire images of the bilateral upper femur in bone tissue windows. The scanning parameters included a slice thickness of 1 mm and an interval of 1 mm, covering a region from 10 cm above the apex of the greater trochanter to the knee joint. The CT data were saved in DICOM format, and the right femur was used for further analysis.

### 2.2 Software

Mimics Research 21.0, Geomagic Wrap, HyperMesh 2019, Creo 6.0, Abaqus 2020 were used for data processing, modeling, and analysis.

### 2.3 Construction of AO 31-A3.3 Femoral Intertrochanteric Fracture Model

The CT image data were imported into Mimics Research 21.0, and the femur was identified using the default “Bone (CT)” threshold. A 3D reconstruction of the right femur was generated using tools such as Edit Masks, Smart Fill, Calculate Part, and Smooth. The reconstructed model was then exported in STL format to Geomagic Wrap, where an AO 31-A3.3 femoral intertrochanteric fracture model was created. This involved remeshing, deleting unnecessary elements, and filling holes to divide the femur into three segments: the femoral head and neck, the lesser trochanter, and the femoral shaft (Figure 1A). The model was further optimized using surface fitting operations and saved in STEP format.

### 2.4 PFNA and PFNA+PHLP Internal Fixation Models

3D models of the PFNA and the PHLP were created and assembled in Creo 6.0 (Figure 1B). Orthotropic cross-sectional views of the PFNA internal fixation were generated to visualize the implant geometry (Figure 1C). The specifics of the internal fixation are shown in Table 1. The A3.3 fracture model, PFNA, and PFNA+PHLP models were assembled in Abaqus 2020 according to surgical standards. The spiral blade was positioned in the middle-lower third of the femoral neck, with its lateral position centered and a tip-apex distance of less than 20 mm. The locking plate was placed on the lateral side of the femur. To facilitate finite element assembly, a hole was created in the middle of the plate using geometric editing tools. A self-locking nail was simulated using coupling and binding commands

to achieve unicortical fixation with three screws at the top and bottom of the plate. The assembled models were imported into HyperMesh 2019 in STEP format for meshing. A 10-node modified quadratic tetrahedral element (C3D10M) with a size of 2 mm was used, and grid convergence was verified. The final models were exported in INP format for analysis (Figure 1D-E). The friction coefficients were defined as follows: 0.46 between bone surfaces, 0.3 between bone and internal fixation, and 0.23 between the spiral blade and the main nail [12].

**Table 1 Details of internal fixation**

| Materials | Models and specifications | Manufacturers |
|---|---|---|
| PFNA | 170 mm in the length of the main nail; 10 mm in the diameter of the spiral blade, 100 mm in length; 130º in the collo-diaphyseal angle of the femur, and 5º in the femoral valgus resection angle. | Suzhou Xinrong Best Medical Instrument Co., Ltd. |
| PHLP | Three-hole plate with a length of 95 mm | Ideal (Suzhou) Medical Instrument Co., Ltd. |

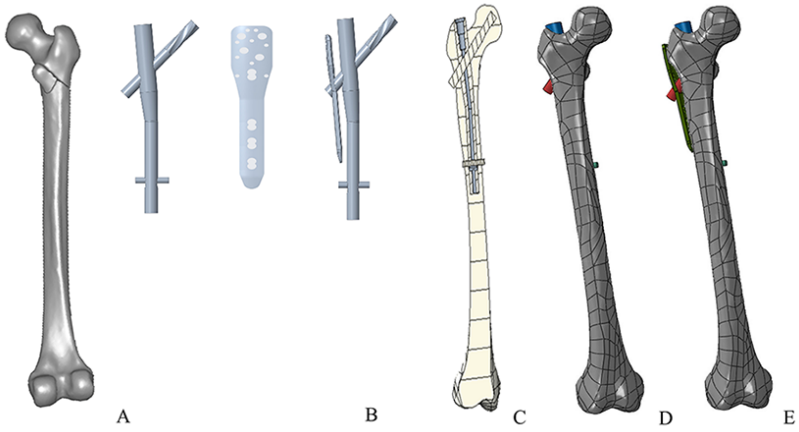


**Figure 1 Finite element simulation models. (A) AO 31-A3.3 femoral intertrochanteric fracture model; (B) PFNA, PHLP, and PFNA+PHLP internal fixation models; (C) Orthotropic cross-sectional view of the PFNA internal fixation model; (D) PFNA and PFNA+PHLP internal fixation assembly models.**

### 2.5 Material Properties and Boundary Conditions

The femoral mesh model of the A3.3 fracture was imported into Mimics Research 21.0 in INP format and divided into 10 material regions based on gray values. Material properties were assigned using the following empirical formulas provided by Mimics: Density = − 13.4+1017 × Gray value, Young's modulus = − 388.8+5925 × Density. The Poisson's ratio was set to 0.3. The material properties of the internal fixation components were defined as follows: Young's modulus = 110 GPa and Poisson's ratio = 0.3 [13, 14]. Boundary conditions were applied as follows: the distal femur was fully fixed, and a reference point (RP-1) was defined on the femoral head's spherical surface. This point was coupled with nodes on the femoral head to apply loads. Based on the volunteer's body weight, static (600 N, 100% body weight) and dynamic (1710 N, 285% body weight) loads were applied in the z-direction to simulate standing and walking at 4 km/h, respectively (Figure 2) [15].


**Figure 2 Schematic representation of loading conditions applied to the models.**

### 2.6 Finite Element Analysis

The Abaqus/Standard solver was used for finite element analysis. The running kernel and memory allocation were configured, and the simulation was executed. The von Mises stress and displacement distributions of the two internal fixation models were calculated. The results were visualized and analyzed using Abaqus 2020 software.

## 3. Results

Analysis of the von Mises stress nephograms (Figure 3) and displacement nephograms (Figure 4) for the two internal fixation models revealed significant differences in biomechanical performance. Under static loading conditions, the maximum von Mises stress for the PFNA internal fixation model was 264.4 MPa, compared to 152.1 MPa for the PFNA+PHLP model, representing a reduction of approximately 40%. In the PFNA model, the maximum stress was concentrated at the contact point between the spiral blade and the main nail. In contrast, the PFNA+PHLP model exhibited maximum stress near the junction of the locking plate and the tail end of the spiral blade. The stress distribution in the femur was more uniform with PFNA+PHLP fixation compared to PFNA fixation.

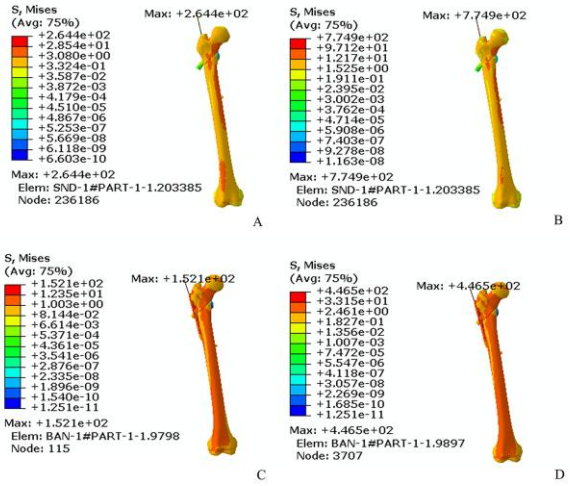


**Figure 3 Von Mises stress distribution nephograms for the two internal fixation models under different loading conditions.(A) Von Mises stress distribution of PFNA under static loading; (B) Von Mises stress distribution of PFNA under dynamic loading; (C) Von Mises stress distribution of PFNA+PHLP under static loading; (D) Von Mises stress distribution of PFNA+PHLP under dynamic loading.**

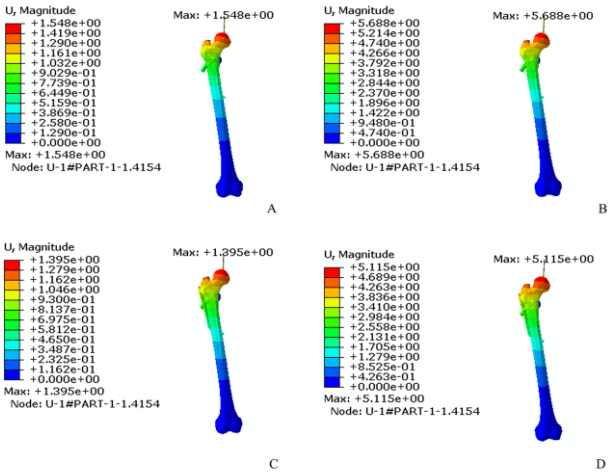


**Figure 4 Displacement distribution nephograms for the two internal fixation models under different loading conditions.(A) Displacement distribution of PFNA under static loading; (B) Displacement distribution of PFNA under dynamic loading; (C) Displacement distribution of PFNA+PHLP under static loading; (D) Displacement distribution of PFNA+PHLP under dynamic loading.**

The maximum displacement for both models occurred at the apex of the femoral head. Under static loading, the displacement was 1.548 mm for the PFNA model and 1.395 mm for the PFNA+PHLP model. Under dynamic loading, the maximum von Mises stress increased to 774.9 MPa for the PFNA model and 446.5 MPa for the PFNA+PHLP model, with the latter showing a reduction of approximately 40%. The locations of maximum stress and displacement under dynamic loading were consistent with those observed under static loading. The maximum displacement under dynamic conditions was 5.688 mm for the PFNA model and 5.115 mm for the PFNA+PHLP model. These results are summarized in Table 2.

**Table 2 Von Mises stress and displacement values for the two internal fixation methods under static and dynamic loading conditions.**

| Internal fixation methods | Von Mises stress under static loading（Mpa） | Von Mises stress under dynamic loading（Mpa） | Displacement under static loading（mm） | Displacement under dynamic loading（mm） |
|---|---|---|---|---|
| PFNA | 264.4 | 774.9 | 1.548 | 5.688 |
| PFNA+PHLP | 152.1 | 446.5 | 1.395 | 5.115 |

Compared to PFNA fixation, PFNA+PHLP fixation significantly reduced stress at the fracture site (including the femoral head, femoral shaft, and lesser trochanter) and at the main nail. Specifically, the von Mises stress at the main nail decreased by approximately 40%, from 15.09 MPa (PFNA) to 9.03 MPa (PFNA+PHLP) under static loading and from 45.35 MPa (PFNA) to 26.98 MPa (PFNA+PHLP) under dynamic loading. In contrast, the von Mises stress in the femoral head, femoral neck, medial wall, and spiral blade showed minimal changes between the two fixation methods (Figure 5).

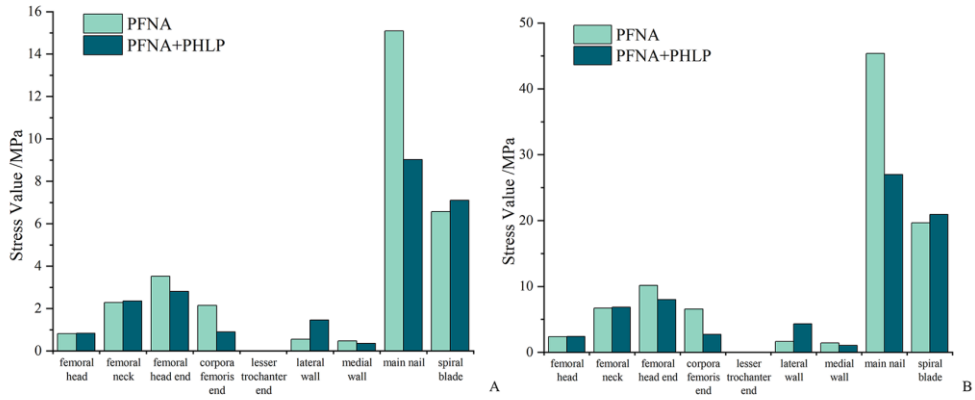


**Figure 5 Comparison of von Mises stress in different regions of the two internal fixation models under different loading conditions.(A) Von Mises stress in each region of PFNA and PFNA+PHLP under static loading; (B) Von Mises stress in each region of PFNA and PFNA+PHLP under dynamic loading.**

The overall displacement of the femoral head, femoral neck, lateral wall, and spiral blade was slightly reduced in the PFNA+PHLP model compared to the PFNA model under both static and dynamic loading conditions. However, these differences were not statistically significant (Figure 6).

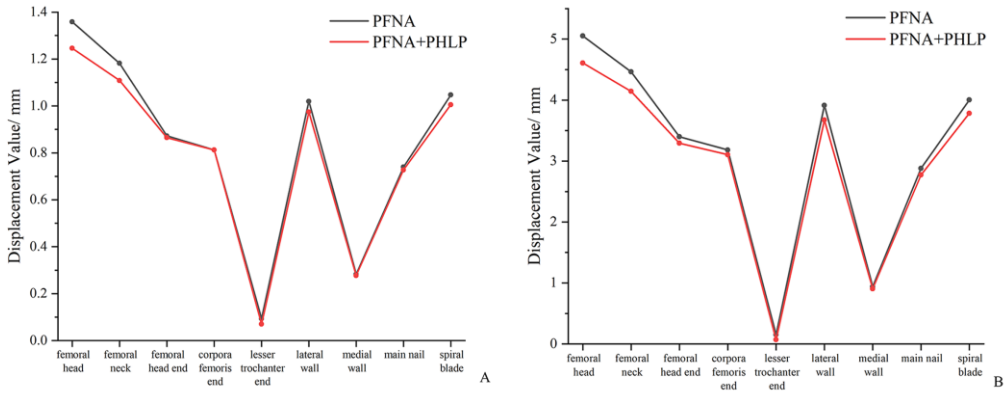


**Fig. 6 Comparison of displacement in different regions of the two internal fixation models under different loading conditions.(A) Displacement in each region of PFNA and PFNA+PHLP under static loading; (B) Displacement in each region of PFNA and PFNA+PHLP under dynamic loading.**

## 4. Discussion

Von Rüden et al. identified the junction of the main nail and the spiral blade as the primary stress concentration area and the weak point of head-neck intramedullary nails [16]. In this study, the maximum von Mises stress in the PFNA fixation model was observed at the contact point between the spiral blade and the main nail, consistent with previous findings. However, in the PFNA+PHLP fixation model, the maximum stress shifted to the junction of the locking plate and the tail end of the spiral blade, with a reduction in stress magnitude of approximately 40% under both static and dynamic loading conditions. This redistribution of stress and the reduction in peak stress values help mitigate the risk of internal fixation failure caused by stress concentration.

Wang Renkai et al. proposed the "five-point stability theory" for femoral intertrochanteric fractures with lateral wall involvement. According to this theory, stability is achieved through a framework formed by the head of the spiral blade, the main nail at the greater trochanter entrance, the proximal and distal ends of the lateral wall fracture, and the distal locking nail. The addition of a lateral plate connecting the proximal and distal femur further enhances fracture stability [17]. In this study, the von Mises stress at the main nail

in the PFNA+PHLP model was reduced by approximately 40% compared to the PFNA model under both static and dynamic loading. Concurrently, the stress on the lateral wall increased, reflecting the load-sharing effect of the locking plate. The von Mises stress on the plate was 11.77 MPa under static loading and 34.76 MPa under dynamic loading, indicating that the plate effectively redistributed stress away from the main nail, resulting in a more balanced stress distribution across the entire fixation system. This reduction in stress at the fracture site further supports the role of lateral wall reconstruction in enhancing fixation stability, consistent with the five-point stability theory. Notably, the stresses on the femoral head, femoral neck, medial wall, and spiral blade remained largely unchanged.

Displacement analysis revealed that the maximum displacements in both fixation models occurred at the apex of the femoral head, with no significant differences between static and dynamic loading conditions. While the PFNA+PHLP model showed slight reductions in displacement at the femoral head, femoral neck, lateral wall, and spiral blade, these changes were not substantial. This suggests that lateral wall reconstruction with PHLP has a limited impact on displacement but significantly improves stress distribution and overall fixation strength.

PFNA intramedullary fixation is widely regarded as the gold standard for femoral intertrochanteric fractures due to its biomechanical advantages and minimally invasive nature. The main nail also functions as a "metal lateral wall," reducing bone mass migration to some extent [18, 19]. However, PFNA fixation is associated with a higher risk of failure in unstable fractures, particularly those involving lateral wall disruption [20, 21]. For such fractures, especially AO 31-A3.3 types, many scholars advocate for primary reconstruction of the lateral wall using nails, Kirschner wires, tension bands, or plates, depending on the fracture pattern. While these methods have demonstrated clinical efficacy, there is a lack of biomechanical data to support their use [22-24].

In this study, we innovatively employed a Proximal Humerus Locking Plate (PHLP) for lateral wall reconstruction, taking advantage of its wider design to provide broader fixation coverage. Preliminary clinical observations indicate that PFNA+PHLP fixation, while associated with slightly longer operative times and increased blood loss compared to PFNA, offers significant advantages in reducing complications such as hip varus and enabling earlier postoperative rehabilitation. These findings suggest that PFNA+PHLP fixation can improve hip joint function and surgical outcomes. However, the sample size of clinical cases is currently limited, and further retrospective studies with larger cohorts are needed to validate these results.

This study represents the first finite element analysis comparing the von Mises stress and displacement distributions of PFNA and PFNA+PHLP fixation under both static and dynamic loading conditions for AO 31-A3.3 femoral intertrochanteric fractures. The results provide valuable biomechanical evidence supporting the use of PFNA+PHLP fixation in clinical practice.

In summary, PFNA+PHLP fixation offers superior fixation strength and more balanced stress distribution compared to PFNA in the treatment of femoral intertrochanteric fractures with lateral wall involvement. This approach may enable earlier postoperative mobilization, reduce complications, and improve patients' quality of life. However, this study has several limitations. The simulation of walking loads was based on constant forces, whereas actual gait involves complex cyclic loading patterns. Additionally, the effects of hip joint reaction forces and surrounding muscle forces were not considered. The bone mineral density and elastic modulus of the femur were derived from empirical formulas, which may not fully reflect real-world conditions. Furthermore, only a single fracture type (AO 31-A3.3) was analyzed. Future studies will optimize the finite element model to incorporate gait cycle loading, muscle forces, and variations in bone mineral density and elastic modulus. These improvements will provide more comprehensive biomechanical insights to guide surgical planning for femoral intertrochanteric fractures with lateral wall fractures.

**Authors' Contributions**

LZ: investigation, methodology, software, funding acquisition and writing–original draft. LW: data curation, formal analysis and writing–original draft. RX : formal analysis, validation and writing–original draft. YB: resources, project

administration, supervision, writing–review and editing. SH: conceptualization, methodology, funding acquisition, writing–review and editing. All authors read and approved the final manuscript.

**Funding**

This work was supported by grants from the the Science and Technology Program of Suzhou (Grant No. SKY2023117) and the Clinical Key Diseases' Diagnosis and Treatment Program of Suzhou (Grant No. LCZX202135).

**Data Availability Statement**

The original contributions presented in the study are included in the article/Supplementary Materials, further inquiries can be directed to the corresponding authors.

**Acknowledgements and Ethical Standards**

I extend my sincere gratitude to my supervisors for their invaluable guidance, colleagues for their support.This study was conducted in compliance with ethical guidelines, and all data were obtained from a healthy volunteer with informed consent. No animal or human trials were involved beyond the use of anonymized CT data.

**Conflicts of Interest**

The authors declare no conflict of interest.

**References**

1. Ju, J.-b., Zhang, P.-x. and Jiang, B.-g. (**2019**), Risk Factors for Functional Outcomes of the Elderly with Intertrochanteric Fracture: A Retrospective Cohort Study. Orthop Surg, 11: 643-652. doi.org/10.1111/os.12512.
2. Buyukdogan, K., Caglar, O., Isik, S., Tokgozoglu, M., Atilla, B. (**2017**). Risk factors for cut-out of double lag screw fixation in proximal femoral fractures. Injury, 48(2), 414–418. doi.org/10.1016/j.injury.2016.11.018.
3. Hsu, C. E., Shih, C. M., Wang, C. C., Huang, K. C. (**2013**). Lateral femoral wall thickness. A reliable predictor of post-operative lateral wall fracture in intertrochanteric fractures. The bone & joint journal, 95-B(8), 1134–1138. doi.org/10.1302/0301-620X.95B8.31495.
4. Wang, J., Ma, J. X., Lu, B., Bai, H. H., Wang, Y., Ma, X. L. (**2020**). Comparative finite element analysis of three implants fixing stable and unstable subtrochanteric femoral fractures: Proximal Femoral Nail Antirotation (PFNA), Proximal Femoral Locking Plate (PFLP), and Reverse Less Invasive Stabilization System (LISS). Orthopaedics and traumatology, surgery and research : OTSR, 106(1), 95–101. doi.org/10.1016/j.otsr.2019.04.027.
5. Palm, H., Jacobsen, S., Sonne-Holm, S., Gebuhr, P. (**2007**). Integrity of the lateral femoral wall in intertrochanteric hip fractures: an important predictor of a reoperation. The Journal of bone and joint surgery. American volume, 89(3), 470–475. doi.org/10.2106/ JB JS.F.00679.
6. Abram, S. G., Pollard, T. C., Andrade, A. J. (**2013**). Inadequate 'three-point' proximal fixation predicts failure of the Gamma nail. The bone and joint journal, 95-B(6), 825–830. doi.org/10.1302/0301-620X.95B6.31018.
7. Haidukewych G. J. (**2010**). Intertrochanteric fractures: ten tips to improve results. Instructional course lectures, 59, 503–509.
8. Erinç, S., Bozca, M. A., Bankaoğlu, M., Çakırtürk, S., Yahşi, Y., Özdemir, H. M. (**2020**). Association of abductor hip muscle atrophy with fall-related proximal femur fractures in the elderly. Injury, 51(7), 1626–1633. doi.org/10.1016/j.injury.2020.04.054.
9. Hao, Y., Zhang, Z., Zhou, F., Ji, H., Tian, Y., Guo, Y., Lv, Y., Yang, Z., Hou, G. **(2019**). Risk factors for implant failure in reverse oblique and transverse intertrochanteric fractures treated with proximal femoral nail antirotation (PFNA). Journal of orthopaedic surgery and research, 14(1), 350. doi.org/10.1186/s13018-019-1414-4.
10. Tarrant, S. M., Graan, D., Tarrant, D. J., Kim, R. G., Balogh, Z. J. (**2021**). Medial Calcar Comminution and Intramedullary Nail Failure in Unstable Geriatric Trochanteric Hip Fractures. Medicina(Kaunas,Lithuania) , 57(4) , 338. doi.org/10.3390/ medicina57040338.
11. Chen, Z. X., Zhou, Z. Y., Liu, F., Yang, F., Wang, C. G. (**2018**). China journal of orthopaedics and traumatology, 31(9), 840–845. doi.org/10.3969/j.issn.1003-0034.2018.09.012.
12. Eberle, S., Gerber, C., von Oldenburg, G., Högel, F., Augat, P. (**2010**). A biomechanical evaluation of orthopaedic implants for hip fractures by finite element analysis and in-

vitro tests. Proceedings of the Institution of Mechanical Engineers. Part H, Journal of engineering in medicine, 224(10), 1141–1152. doi.org/10.1243/09544119JEIM799.
13. Yosibash, Z., Padan, R., Joskowicz, L., Milgrom, C. **(2007)**. A CT-based high-order finite element analysis of the human proximal femur compared to in-vitro experiments. Journal of biomechanical engineering, 129(3), 297–309. doi.org/10.1115/1.2720906.
14. Jiang-Jun, Z., Min, Z., Ya-Bo, Y., Wei, L., Ren-Fa, L., Zhi-Yu, Z., Rong-Jian, C., Wei-Tao, Y., Cheng-Fei, D. (**2014**). Finite element analysis of a bone healing model: 1-year follow-up after internal fixation surgery for femoral fracture. Pakistan journal of medical sciences, 30(2), 343–347. 15.
15. Bergmann, G., Deuretzbacher, G., Heller, M., Graichen, F., Rohlmann, A., Strauss, J., Duda, G. N. (**2001**). Hip contact forces and gait patterns from routine activities. Journal of biomechanics, 34(7), 859–871. doi.org/10.1016/s0021-9290(01)00040-9 16.
16. Von Rüden, C., Hungerer, S., Augat, P., Trapp, O., Bühren, V., Hierholzer, C. (**2015**). Breakage of cephalomedullary nailing in operative treatment of trochanteric and subtrochanteric femoral fractures. Archives of orthopaedic and trauma surgery, 135(2), 179–185. doi.org/10.1007/s00402-014-2121-6.
17. Wang, R., Zhang, H., Wei, Q., Ding, C., Cao, L., Yi, M., Tong, D., Li, D., Fan, Z., Wu, D., Ji, F., Tang, H. (**2021**). Intramedullary nails in combination with reconstruction plate in the treatment of unstable intertrochanteric femoral fractures with lateral wall damage. International orthopaedics, 45(11), 2955–2962. doi.org/10.1007/s00264-021-05004-6.
18. Kim, Y., Bahk, W. J., Yoon, Y. C., Cho, J. W., Shon, W. Y., Oh, C. W., Oh, J. K. (**2015**). Radiologic healing of lateral femoral wall fragments after intramedullary nail fixation for A3.3 intertrochanteric fractures. Archives of orthopaedic and trauma surgery, 135(10), 1349–1356. doi.org/10.1007/s00402-015-2284-9.
19. Guo, Y., Yang, H. P., Dou, Q. J., He, X. B., Yang, X. F. (**2017**). Efficacy of femoral nail anti-rotation of helical blade in unstable intertrochanteric fracture. European review for medical and pharmacological sciences, 21(3 Suppl), 6–11.
20. Kanakaris, N. K., Noviello, C., Saeed, Z., Mitrogiannis, L., Tosounidis, T. H., Tartaglia, N. (**2015**). Preliminary results of the treatment of proximal femoral fractures with the AFFIXUS nail. Injury, 46 Suppl 5, S12–S17. doi.org/10.1016/j.injury.2015.08.007 .
21. Jiménez Díaz, V., Auñón Martín, I., Pardo García, J. M., Olaya González, C., Caba Doussoux, P. (**2021**). Does the fracture of the lateral wall affect the degree of collapse and the degree of sliding of the cephalic plate, in pertrochanteric fractures treated by intramedullary interlocking? Radiological study and review of the literature. Revista espanola de cirugia ortopedica y traumatologia (English ed.), 65(2), 108–115. doi.org/10.1016/j.recot.2020.06.013.
22. Gao, Z., Lv, Y., Zhou, F., Ji, H., Tian, Y., Zhang, Z., Guo, Y. (**2018**). Risk factors for implant failure after fixation of proximal femoral fractures with fracture of the lateral femoral wall. Injury, 49(2), 315–322. doi.org/10.1016/j.injury.2017.11.011.
23. Rajput, A. K., Gupta, P. K., Gill, S. P. S., Singh, S. K., Raj, M., Singh, J., Dubey, P., Sharma, P. (**2022**). Prospective Comparative Study Between Proximal Femoral Nail vs. Screw Augmented Proximal Femoral Nail in Unstable Intertrochanteric Fractures of Femur. Cureus, 14(12), e32791. doi.org/10.7759/cureus.32791.
24. Gupta, A., Bansal, H., Kumar, A., Mittal, S., Trikha, V. (**2020**). The effect on outcomes of the application of circumferential cerclage cable following intramedullary nailing in reverse intertrochanteric femoral fractures. European journal of orthopaedic surgery & traumatology : orthopedie traumatologie, 30(5), 949. doi.org/10.1007/ s005 90-020-02641-2.